JOURNAL OF MATERIALS SCIENCE **36** (2001) 5073–5078

Fracture behaviour of virgin and recycled isotactic polypropylene

J. AURREKOETXEA*, M. A. SARRIONANDIA, I. URRUTIBEASCOA
Departement of Mechanics, Faculty of Engineering, Mondragon Unibertsitatea, 20500 Mondragon, Spain
E-mail: jaurrekeotxea@eps.muni.es

M. LI. MASPOCH
Dept. Ciència dels Materials i Eng. Met. Centre Català del Plàstic, Universitat Politècnica de Catalunya, C/Colom 114, 08222 Terrassa, Barcelona, Spain

Fracture behaviour of virgin and six times recycled isotactic polypropylene (PP) has been studied. Instrumented Charpy impact tests have been carried out to characterise the fracture parameters and scanning electron microscopy was used to study the fracture surfaces. Recycled PP presents slightly smaller spherulites and lower fracture toughness than virgin one. Fractography analysis reveals that crazing is the dominant fracture micromechanism for both materials, and that the difference in fracture toughness is a consequence of the smaller plastically deformed volume at the notch tip of the recycled polypropylene.

1. Introduction

The last thirty years plastic materials consumption, and consequently plastic waste production, has experienced a spectacular growth. Furthermore, the environmental awareness has also risen to the point that waste is perceived as a problem of today's society. Thus, now more than ever, industry has to be concerned with waste reduction strategies. It is well known that reprocessing, also called primary recycling [1], is carried out extensively in the plastic industry. Primary recycling focuses on clean, uncontaminated, single type scrap from processing operations.

The fact that polypropylene (PP) is a polymer with a high production volume makes recycling especially interesting for economical and environmental reasons. PP undergoes severe thermo-mechanical degradation phenomena during processing due to the effect of high temperatures and intensive shearing [2–6]. In a previous paper [7] the effects of recycling on the structure and the mechanical properties of isotactic polypropylene were investigated. The absence of changes in the chemical structure and the increase of the Melt Flow Index (MFI) suggested that chain scission, and not oxidation, was the dominant degradation mechanism under the experimental conditions. The observed reduction of the molecular weight with recycling increased the mobility and the ability to fold of the chains, allowing the formation of thicker lamellae and higher degree of crystallinity. The crystallisation rate and the apparent crystallisation temperature also increased with recycling.

The aim of this paper has been to determine the effects of recycling on the fracture behaviour of PP. The fracture behaviour of a material, which depends among others on morphological variables, sets limits both to design and safety of engineering components. In the present work, six times injection moulded PP has been taken as the representative recycled PP. Changes in spherulitic morphology were studied. Fracture behaviour of the virgin and recycled material was characterised by instrumented Charpy impact tests. In order to obtain further information about the extent of plastic deformation and mode of failure, fracture surfaces were studied by scanning electron microscopy.

2. Experimental procedure

2.1. Materials and specimen preparation

For this investigation a commercial isotactic polypropylene (PP) homopolymer injection grade (SM6100, Montell) was used. To simulate the recycling cycle, PP was processed in a Battenfeld BA 600CDC injection moulding machine, and the tensile test specimens obtained were granulated in a knife mill for the next recycling cycle. This procedure was repeated up to six times. A melt temperature of 200°C and a cooling time of 20 s were used in accordance with practice ASTM D-4101-96a. The injection pressure was fixed at 594 bar following the procedure described in ASTM D-1897-81. The injection time and the screw rotation rate used were 0.43 s and 200 rpm respectively. These injection parameters were maintained for all the recycling cycles. The virgin PP is referred to as VPP and the six times recycled one as RPP.

Prismatic bars (ASTM D-647) with 12.7 mm × 6.35 mm × 127 mm dimensions and using the injection

*Author to whom all correspondence should be addressed.

parameters described above were injection moulded. These bars were cut to 12.7 mm × 6.35 mm × 63.5 mm dimensions and notched to obtain single edge notched bend (SENB) specimens for impact tests. Crack length (a) to depth (W) ratios between 0.3 and 0.54 were used. A pre-crack was also introduced by sliding a fresh razor blade over the tip of the notch. The final value of the notch depth was measured after fracture by using an optical microscope. The SENB specimens were annealed in a fan-assisted oven for 3 h at 150°C.

2.2. Characterisation of the microstructure

Samples for the spherulitic morphology study were taken from the core of the Charpy specimens. The flat surface was polished with several emery papers, and finally with a very fine diamond powder (1 μm) until no residual scratches were visible. The specimens were etched in an ultrasonic bath. The solution consisted of a 1 : 1 volume mixture of sulphuric and phosphoric acids ($H_2SO_4 + H_3PO_4$) with 0.7% by weight potassium permanganate [8]. Etched pieces were then rinsed several times with distilled water, hydrogen peroxide and finally with acetone, in order to avoid any artefacts caused by pollution effects. The above operations resulted in the amorphous part of the spherulites being etched preferentially, and thus the substructure could be studied by direct observation with a scanning electron microscopy.

2.3. Mechanical properties

SENB specimens were tested on a CEAST instrumented Charpy impact pendulum, equipped with a data acquisition unit. Impacting of the specimens occurred under the following conditions: mass of the striker = 2.182 kg, $v = 0.57$ m/s, room temperature, span 50.8 mm. Data acquisition was made with a time interval of 2 μs per point. The impact data were analysed according to the linear elastic fracture mechanics approach (LEFM) [9]. The fracture toughness (K_{IC}) was calculated by means of the equation

$$K_{IC} = \frac{3}{2} \cdot \frac{F_{max} \cdot S}{B \cdot W^{3/2}} \cdot (a/W)^{1/2} \cdot Y(a/W) \quad (1)$$

where F_{max} is the maximum load; S the span; B and W are the thickness and the width of the specimen, respectively; a is the initial crack length and $Y(a/W)$ a calibration factor depending on the specimen geometry.

For the determination of the critical strain energy release rate (G_{IC}), the following equation was used

$$G_{IC} = \frac{U_c}{BW\phi} \quad (2)$$

where U_c is the fracture energy and ϕ is a calibration factor which depends on the length of crack and the size of the sample.

In order to ensure plane-strain conditions the dimensions of the specimen should fulfil the following condition

$$(W - a), B, a \geq 2.5(K_{IC}/\sigma_y)^2 = A_c \quad (3)$$

where σ_y is the yield stress and A_c is the plain strain verification factor.

In the case of LEFM a simple relationship exists between G_{IC} and K_{IC}, under plane-strain conditions, this relationship is given by

$$G_{IC} = \left(\frac{K_{IC}^2}{E}\right)(1 - \nu^2) \quad (4)$$

where ν is Poisson's ratio, taken to be 0.3.

Prismatic specimens without notches were used in low energy impact tests. The impact elastic modulus (E_{impact}) was calculated as follows

$$E_{impact} = \frac{S^3}{4BW^3} \cdot \left[\frac{F}{d}\right] \cdot \left[1 + 2.85\left(\frac{W}{S}\right)^2 - 0.84\left(\frac{W}{S}\right)^3\right] \quad (5)$$

where $[\frac{F}{d}]$ is the initial slope of the load-displacement curve.

2.4. Fractography

Fracture surfaces of tensile and Charpy specimens were studied by scanning electron microscopy (SEM) in order to determine the micromechanisms of fracture. Direct observation of the fracture surfaces was carried out under low vacuum conditions (20–25 Pa).

3. Results and discussion

3.1. Characterisation of the microstructure

There are several reports in the literature claiming that the spherulitic architecture of PP plays a major role in altering the failure behaviour [10–12]. However, the effects of spherulitic size are difficult to distinguish from those of percent crystallinity, lamellar thickness, or tie-molecule density [13].

Virgin and recycled PP present the same α-spherulitic morphology (Fig. 1a). Recycling has two antagonistic consequences on the spherulite size; the impurities introduced during the recycling cycle have a positive effect, since they act as heterogeneous nuclei and reduce the average diameter. The negative effect is due to the nuclei destruction during injection moulding caused by the high temperature and shearing [14]. It seems that under our experimental conditions the effect of the additional foreign nuclei is not overshadowed by the temperature-shearing nuclei destruction, and the average spherulite diameter of the virgin PP is slightly larger than that of the recycled one, 72 ± 11 μm and 46 ± 6 μm respectively. This result correlates well with the crystallisation results reported in a previous paper [7], where the recycled PP showed higher nucleation rate.

As can be observed in Fig 1b the connection between the spherulites is good, with a high density of inter-spherulitic links at the boundaries.

TABLE I Tensile elastic modulus (E), yield stress (σ_y) and elongation at break (ε_b), degree of crystallinity (X_c) and Melt Flow Index (MFI) for virgin (VPP) and six times recycled PP (RPP)

Sample	E[MPa]	σ_y [MPa]	ε_b [%]	X_c [%]	MFI [g/10 min]
VPP	1704 ± 39	34.7 ± 0.22	66.37 ± 5.38	44.6	10.83 ± 0.86
RPP	1993 ± 49	36.33 ± 0.17	51.55 ± 2.2	48.5	13.37 ± 0.64

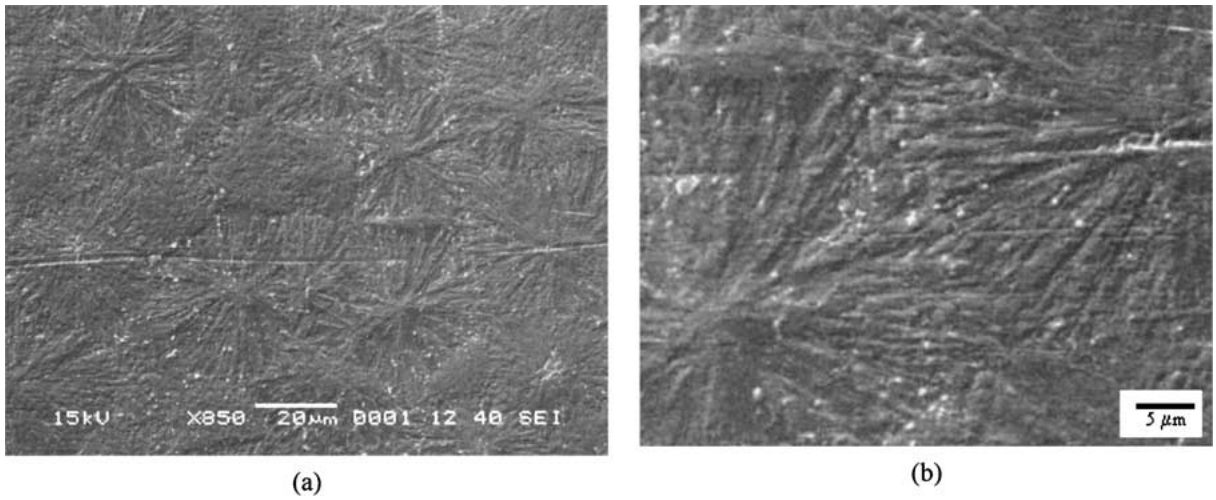

Figure 1 Spherulitic morphology of the PP (a), and interspherulitic boundary (b).

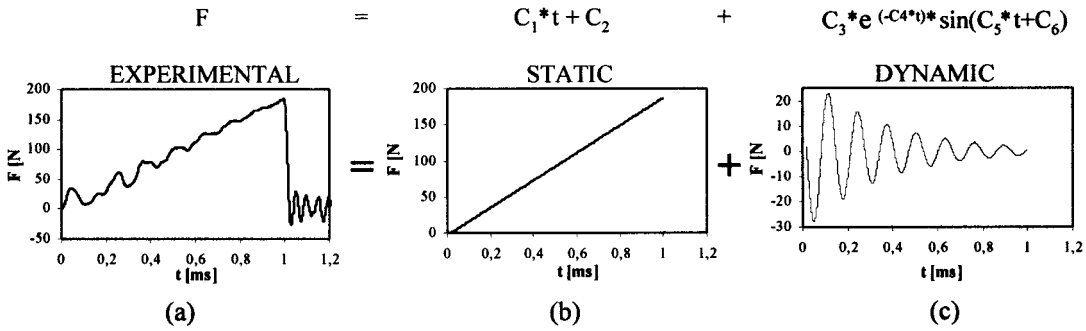

Figure 2 Impact test F-t experimental curve (a), it has been divided in static (b) and dynamic (c) contributions.

3.2. Tensile test

In a previous paper [7] we have shown that recycling increases the elastic modulus and yield stress due to the higher degree of crystallinity of the recycled materials. However, the elongation at break decreases with recycling as a consequence of the reduction of the molecular weight, expressed in higher Melt Flow Index (MFI). The values of these parameters are summarised for virgin (VPP) and six times recycled PP (RPP) in the Table I.

3.3. Impact test

Fig. 2 displays a characteristic (F, t) experimental curve for VPP. All VPP and RPP specimens fractured brittlely, Charpy specimens broke instantaneously after the maximum load was reached and at small deflections. The (F, t) trace displays superimposed load oscillations. Essentially, this behaviour is associated with the dynamic effects arising from the motion of the specimen [15]. The risk of error in determining the maximum force is negligible, since the dynamic effects are attenuated before the fracture point is reached. However, dynamic effects can cause serious errors in the determination of fracture energy (U_c), as the maximum area under the curve will be mistaken. In order to eliminate these effects, the experimental curves have (Fig. 2a) been fitted with a function composed by static (Fig. 2b) and dynamic (Fig. 2c) contributions. (U_c) has been calculated by taking the area under the static function.

The values of A_c, K_{IC}, G_{IC}, E_{impact} and $G_{ICtheor}$ for VPP and RPP are given in Table II. The fracture values correspond to plane-strain conditions, since both materials fulfil the criteria given by Equation 3. It can be seen that the fracture parameters are slightly lower and the elastic modulus is higher for RPP. The improved impact elastic modulus is probably related, as for tensile results, to the higher crystallinity (Table I) of the RPP. It can also be seen that the value for G_{IC} calculated from Equation 4 and the experimentally determined one are slightly different, indicating that the measure of G_{IC} should be interpreted carefully. In order to explain the worsening of the fracture parameters, analysis of the mechanisms of deformation and fracture should be carried out.

Fig. 3 shows a typical fracture surface (at low magnification) of a VPP sample, this fracture morphology

TABLE II Plane strain verification factor (A_c), fracture toughness (K_{IC}), critical strain energy release rate (G_{IC}), rebound elastic modulus (E_{impact}) and theoretical critical strain energy release rate ($G_{ICtheor}$) for the virgin (VPP) and six times recycled PP (RPP)

Sample	A_c[a][mm]	K_{IC} [MPa $m^{1/2}$]	G_{IC} [KJm^{-2}]	E_{impact} [MPa]	$G_{ICtheor}$ [KJm^{-2}]
PP–R1	5.2	2.23 ± 0.09	2.07 ± 0.05	1995 ± 19	2.27 ± 0.02
PP–R6	4	1.96 ± 0.1	1.96 ± 0.07	2035 ± 40	2.22 ± 0.04

[a]The calculations have been made with yield stress data taken from [16]; $\sigma_y = 49$ MPa at a test speed of 0.6 mm/s.

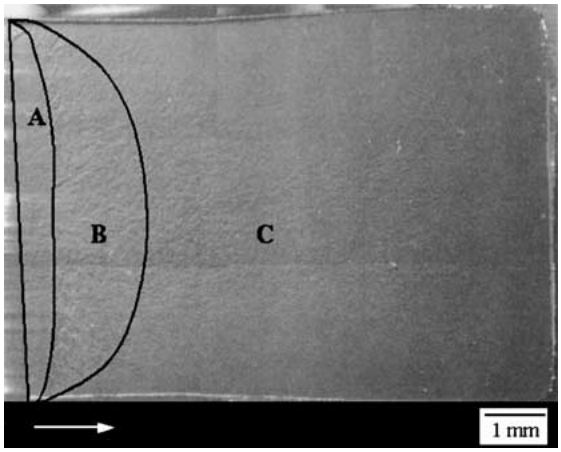

Figure 3 Fracture surface morphology of a Charpy impact test specimen; (A) fracture induction area, (B) rough zone and (C) smooth surface. The arrow indicates the crack propagation direction.

is characteristic of virgin and recycled materials. The micrograph reveals that the fracture surface is relatively smooth and of a brittle appearance. However, plastic deformation is localised in the region close to the notch tip of the impact specimen. In the centre of the specimen the plastically deformed area had propagated further ahead than at the edges of the crack front, an indication of the more critical three-dimensional stress-state generated in the interior of the material. Thus fracture surfaces show three distinct zones. A fracture induction area at the notch tip (A). Beyond the fracture induction area there is a rough zone (B). The remainder of the fracture surface is smooth (C), reflecting unstable crack propagation.

Fig. 4a shows higher magnification scanning electron micrographs of the zone ahead of the notch tip; the appearance of this zone is identical for virgin and recycled PP. This region is called the fracture induction area [17], and is where the material breaks in a ductile manner. The presence of this zone suggests that the precursor to the crack growth is the formation of a large number of crazes [18, 19]. Even if crazing is a characteristic deformation mechanism of glassy polymers, it is very usual in semicrystalline polymers to name crazing the local instability deformation accompanied simultaneously by fibrillation and cavitation. The rupture of the fibrils of the crazes at this region leads to crack nucleation [19, 20], and to catastrophic brittle fracture. The process results in a patchwork structure of residual craze matter on the final fracture surface.

In Fig. 4b remnants of microfibrils of a previously voided, crazed region can be observed. These fibrils seem to be broken up under heat influence [21]. At high load rates the plastic deformation process at the crack tip is adiabatic [22], and a localised temperature rise may occur. That is the reason why the surface does not reflect the usual craze remnants (being "overwritten" by the heat effects).

Spherulite boundaries are of great importance in order to understand the fracture behaviour of PP, since failure of polymers is often initiated on these spots. Here cracks and voids may form during the crystallisation due to some contraction. The "weak site" of boundaries is also derived from the fact that the majority of the non-crystallising component is accumulated in these regions [23]. Another determining factor is the interspherulitic connection by the tie-molecules. These molecules are incorporated in two or more crystals, act as local transmitters of stress between crystallites and are broken during deformation and fracture. The density of tie-molecules decreases with increasing crystallisation temperature [18] and lowering the molecular weight [24]. The fact that crazes develop and propagate within the spherulites (Fig. 4c) indicates that the spherulite boundaries are sufficiently linked to sustain large deformation. Thus, even if RPP has lower molecular weight and higher apparent crystallisation temperature than VPP, the intraspherulitic crack propagation pathway points out that the tie-molecule density at the spherulite boundaries is very similar for both materials.

The micrographs shown in Fig. 5 are representative of the rough zone and the region furthest from the notch tip of VPP, RPP exhibits the same appearance at these two zones. Fig. 5a shows the topology of the fracture surface at the rough zone. Gensler *et al*. [25] have reported that the deformation mechanisms at the notch tip change with the loading rate, and that at intermediate rates (50–1000 mm/s) crazing is the dominant feature. The surface roughness itself was thought to be due to the superposition of different multiple cracks, initiating within the crazes at different times and in slightly different planes. The fracture surface at the region furthest from the notch tip (Fig. 5b) is less rough than at the fracture induction area and rough zone. This implies that plastic deformation occurs only in a localised region at the crack tip, and that the energy absorbed by the material is basically confined to this region.

Fig. 6 shows the fracture induction and rough areas of VPP (Fig. 6a) and RPP (Fig. 6b); VPP has a slightly larger plastically deformed area than RPP. It has been reported that the crazed damage zone ahead of the notch can be initiated more easily in a lower-yield-stress material [17]. Otherwise, the volume of material

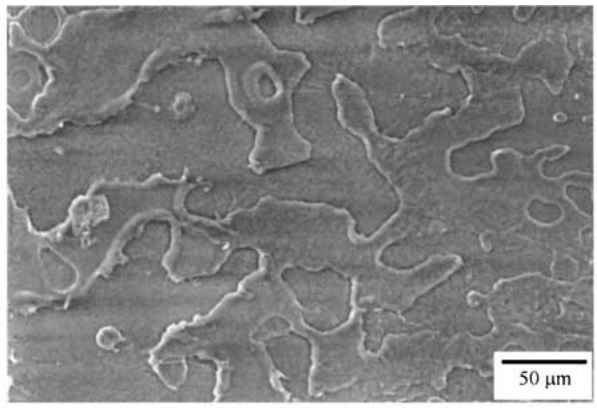

(a)

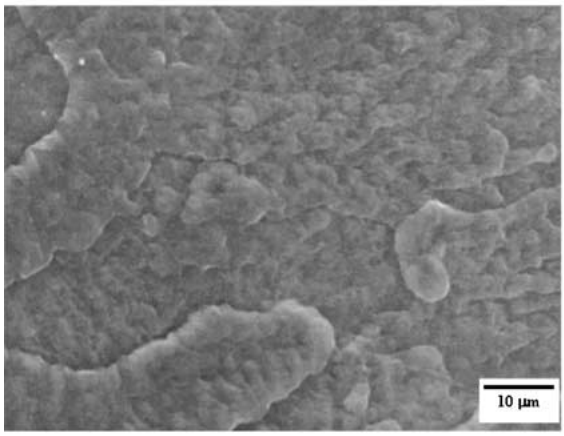

(b)

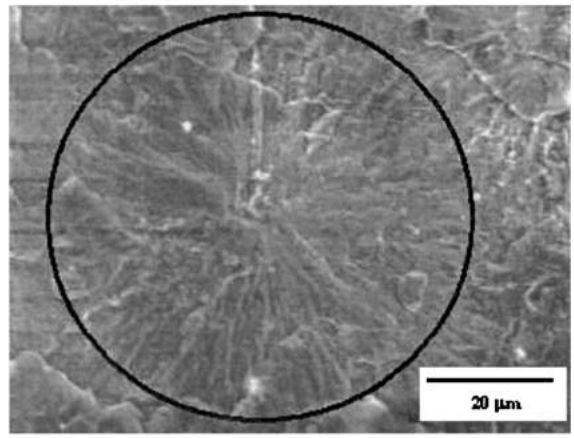

(c)

Figure 4 Scanning electron micrographs taken at the fracture induction area, (a) patchwork structure, (b) remnants of microfibrils of a previously crazed region, (c) intraspherulitic crack propagation pathway.

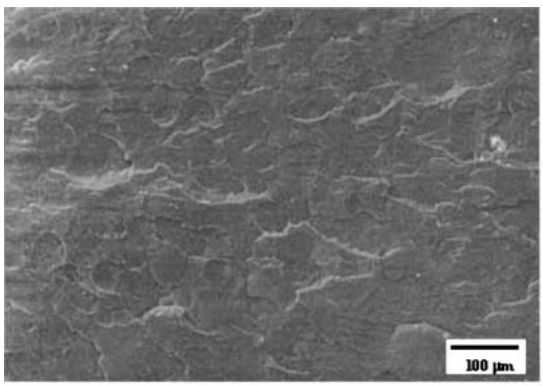

(a)

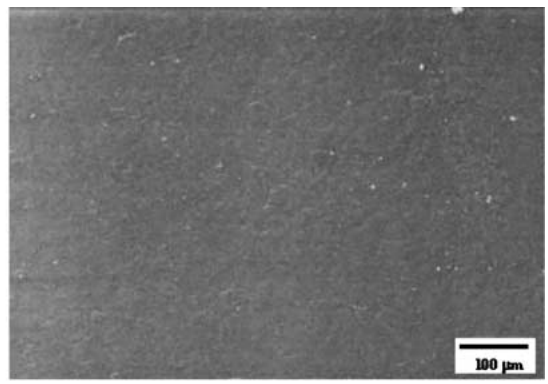

(b)

Figure 5 Scanning electron fractographs taken at the rough zone (a) and at the region furthest from the notch tip (b) of VPP, RPP exhibits the same appearance.

deformed by crazing increases when the degree of crystallinity decreases [20], since the amount of amorphous interlayers in which craze nucleation can take place is enhanced.

Fracture surface observation reveals that crazing is the dominant feature of deformation in virgin and recycled PP. Crazing provides a mechanism for energy dissipation [20]. Thus, fracture toughness increases with increasing the size of the plastically deformed zone. Furthermore, the higher molecular weight of the virgin PP leads to stronger fibrils, which can grow to greater length, and the forces transmitted by the fibrillated region are enhanced. The higher toughness revealed by the virgin PP is attributed to its lower degree of crystallinity (see Table I) and improved strength of the fibrils of the craze.

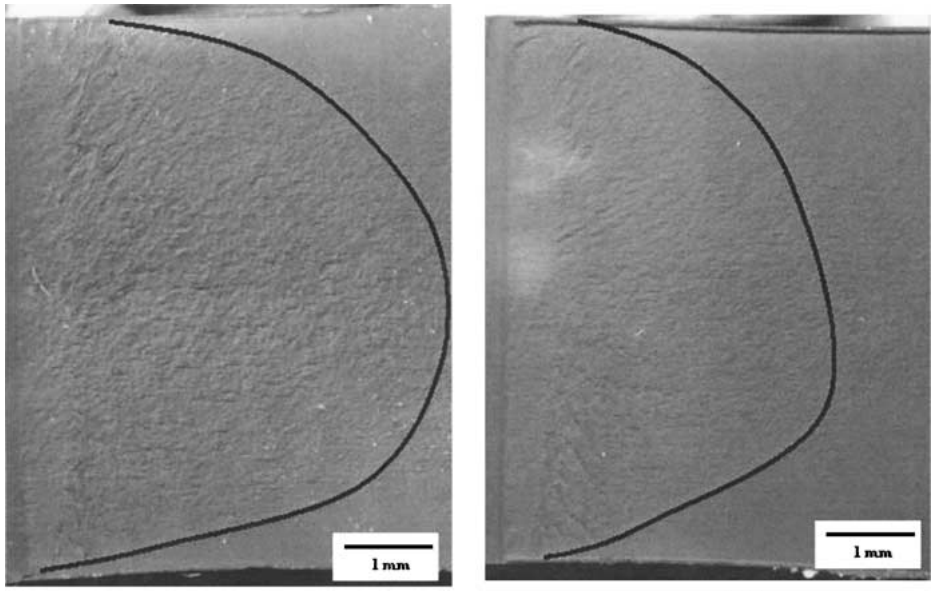

Figure 6 Fracture induction and rough areas of the VPP (a) and RPP (b).

4. Conclusion

The fracture behaviour of virgin and recycled PP has been investigated. Recycling reduces the spherulite size since the quantity of heterogeneous nuclei introduced as impurities is greater than the nuclei destroyed by the high temperature and shearing inherent in injection moulding.

The values of K_{IC} and G_{IC} for the recycled PP are lower than for the virgin PP. Fracture surface observation has revealed that the main micromechanism of fracture for virgin and recycled PP is crazing, which leads to the nucleation and unstable propagation of cracks. The size of the plastically deformed area, and consequently the absorbed fracture energy, is larger for the virgin than for the recycled PP. This is due to the lower degree of crystallinity of the former. Furthermore, the greater molecular weight of the virgin material leads to larger number of crazes and their resistance to break is enhanced, resulting in improved fracture toughness.

Acknowledgements

The authors would like to thank Dr. W. Tato (Manufacturing Department, Mondragon Unibertsitatea) for his helpful discussions, and Dr. O. Santana of Centre Català del Plàstic for his help with the fracture tests.

References

1. C. D. PAPASPYRIDES and J.G. POULAKIS, in "The Polymeric Materials Encyclopedia," edited by J. C. Salomone (CRC Press, Inc, 1996) p. 7403.
2. V. A. GONZÁLEZ GONZÁLEZ, G. NEIRA-VELÁZQUEZ and J. L. ANGULO SÁNCHEZ, *Polym. Degrad. Stab.* **60** (1998) 33.
3. B. E. TIGANIS, R. A. SHANKS and Y. LONG, *J. Appl. Polym. Sci.* **59** (1996) 663.
4. Q. YING, Y. ZHAO and Y. LIU, *Makromol. Chem.* **192** (1991) 1041.
5. V. M. GOL'DBERG and G. E. ZAIKOV, *Polym. Degrad. Stab.* **19** (1987) 221.
6. H. HINSKEN, S. MOSS J. R. PAUQUET and H. ZWEIFEL, *ibid.* **34** (1991) 279.
7. J. AURREKOETXEA, M. A. SARRIONANDIA, I. URRUTIBEASCOA and M. LL. MASPOCH, *J. Mater. Sci.*, in press.
8. R. H. OLLEY and D. C. BASSETT, *Polymer* **23** (1982) 1707.
9. J. G. WILLIAMS, "Fracture Mechanics of Polymers" (Ellis Horwood, Chichester, 1987).
10. J. L. WAY, J. R. ATKINSON and J. NUTTING, *J. Mater. Sci.* **9** (1974) 293.
11. K. FRIEDRICH, *Progr. Colloid Polymer Sci.* **64** (1978) 103.
12. M. OUEDERNI and P. J. PHILLIPS, *J. Polym. Sci. B Polym. Phys.* **33** (1995) 1313.
13. M. SUGIMOTO, M. ISHIKAWA and K. HATADA, *Polymer* **36** (1995) 3675.
14. Z. BRATCZAK, A. GALESKI, E. MASTRUCELLI and H. JANIK, *ibid.* **26** (1985) 1843.
15. J. F. KALTHOFF, *Int. J. Fract.* **27** (1987) 277.
16. A. VAN DER WAL, Ph.D thesis, University of Twente, 1996.
17. S. C. TJONG, J. S. SHEN and R. K. Y. LI, *Polymer* **37** (1996) 2309.
18. R. GRECO and G. RAGOSTA, *J. Mater. Sci.* **23** (1988) 4171.
19. A. O. IBHADON, *J. Appl. Polym. Sci.* **69** (1998) 2657.
20. K. FRIEDRICH, in "Crazing in Polymers," edited H. H. Kausch (Springler-Verlag, Berlin, 1983) p. 225.
21. J. KARGER-KOCSIS, J. VARGA and G. W. EHRENSTEIN, *J. Appl. Polym. Sci.* **64** (1997) 2057.
22. A. VAN DER WAL, J. J. MULDER, H. A. THIJS and R. J. GAYMANS, *Polymer* **39** (1998) 5467.
23. J. VARGA, *J. Mater. Sci.* **27** (1992) 2557.
24. M. ISHIKAWA, K. USHUI, Y. KONDO, K. HATADA and S. GIMA, *Polymer* **37** (1996) 5375.
25. R. GENSLER, C. J. G. PLUMMER, C. GREIN and H. H. KAUSCH, *ibid.* **41** (2000) 3809.

Received 10 April
and accepted 16 May 2001